How seismic anisotropy changes with scale

Dawin Baden, Pierre Henry, Ginette Saracco, Lionel Marié, Alain Tonetto, Yves Guglielmi, Seiji Nakagawa, Gérard Massonnat, Jean-Paul Rolando

How seismic anisotropy changes with scale

Dawin Baden, Pierre Henry, Ginette Saracco, Lionel Marié, and Alain Tonetto, Aix-Marseille Université, CNRS, CEREGE, IRD; Yves Guglielmi, and Seiji Nakagawa, Lawrence Berkeley National Laboratory; Gérard Massonnat, Jean-Paul Rolando, Total Exploration & Production*

Summary:

Physical properties of carbonate rocks cannot be fully captured from laboratory-sized samples. Indeed, heterogeneous facies distribution and/or diagenetic alterations may lead to significant variations in petrophysical properties within few meters. In carbonates, diagenetic transformations are tightly related to nature of fluids flowing through the formations, e.g. via fractures network. Consequently, reservoir properties may have patchy distribution, and may not be correlatable (e.g. using facies distribution or wells-logs correlations) within few meters. Our works aim at characterizing carbonates anisotropy at different scales, and are subject of two presentations at SEG's 87th Annual Meeting. This abstract deals with the second part of our approach, that's to say characterizing impact of diagenetic alteration on reservoir properties and seismic anisotropy, from centimeter to multi-meter scale. This part of the works integrate data from centimeter-scale (mini-cores), decimeter-scale (5" cores), multi-meter (ultrasonic crosshole), and hectometer-scale (seismic), which have been measured at suitable frequency ranges (1MHz, 250kHz, 50kHz, and 1–100Hz, respectively). Although anisotropy is measureable at every scales, its origins vary according to scale. In this study, it is shown that matrix of porous samples are weakly anisotropic as a result of minerals orientation, and inter-crystalline pores. At centimeter-scale, anisotropy can also be related to: (1) patchy distribution of some physical properties, (2) local cracks distribution, and (3) thick single fractures. The lack of correlation between stiffness components from seismic-scale measurements, and laboratory to multi-meter scale ones emphasizes the fact that, when fracturing dominates, measured anisotropy is dominated by fracture/fault related anisotropy and matrix-related anisotropy may be lost. So that, scale effect must be handled carefully in anisotropy analyses, especially for carbonate formations.

Introduction:

This study is consecutive to a series of published works aiming at characterizing both reservoir and elastic properties of Lower Cretaceous limestone from the Urgonian platform of Provence (SE, France). References describing the characteristics of this platform in terms of facies, and biostratigraphy are available e.g. (Leonide et al. 2012). These microporous bioclastic limestones are analogues of different hydrocarbon reservoirs in Middle East, e.g. Kharaib and Shuaiba formations (Borgomano et al. 2013). In addition, several published databases document coupled porosity, and elastic waves velocities measurements from the Urgonian platform (Fournier and Borgomano 2009; Fournier et al. 2011; Fournier et al. 2014; Borgomano et al. 2013). In these works, the authors used conventional laboratory approach, i.e. velocity measurements carried out on 1" to 1.5" mini-cores, under effective stress; and they discussed "*effective media theory*", and the concept of "*pore aspect ratio*" extensively. Nevertheless, a known limitation of these approaches is the implicit assumption of medium's isotropy. Despite this assumption is generally true at plug scale, it is rarely the case at larger scale. Carbonate rocks are often fractured and may have either "*facies-related"* or *"patchy"* porosity distribution that may lead to seismic anisotropy.

The works presented here focus on the impact of up-scaling onto elastic properties of carbonates rocks. Ultrasonic measurements have been carried out onto laboratory-sized samples, and the results are compared to published works, and to our crosshole acoustic survey (cf. our first presentation).

Geological context:

The studied formations are located within vadose zone of *"Fontaine de Vaucluse"* aquifer system. LSBB (Low Noise Underground Laboratory) GAS-gallery gives access to the 30° southward-dipping layers, and five vertical fully-cored boreholes (~20m deep) were drilled as part of previous works (Jeanne 2012; Jeanne, Guglielmi, and Cappa 2013; Jeanne, Guglielmi, and Cappa 2012; Jeanne et al. 2012).

The present study focuses on analyzing elastic properties of six 5" cores (C01 to C06), which are representative of different layers intersected by the boreholes (Figure 1). The facies sampled are inner-platform facies i.e. low to moderate energy, muddy or peloidal carbonate sands with abundant rudists. Cores analyses emphasized two facies groups:

(1) Calcarenites (grainstone to rudstone),
(2) Calcilutites (wackestone to packestone).

Reservoir properties of this facies are related to diagenesis (Léonide et al. 2014), hence, we do not describe them any further in this abstract, instead, we give extensive description of two cores selected to exemplify our works (i.e. C03 & C04). **C03** was selected because it shows gradual transition within a same facies. It is a bioclastic grainstone to rudstone with abundant centimeter scaled rudists fragments and foraminifera. The transition is materialized by the relative abundance of macroscopic bioclasts (rudists), the top of C03 has higher density of macroscopic fragments, whereas bottom has only sand scaled bioclasts. We did not observe any variations in the matrix, and thin sections show large rudists fragments packed into a fine grained matrix, the grains size is <300µm, and the

matrix texture ranged from packestone to grainstone (Figure 2). The micrite in C03 is compact, with low intercrystalline pores. Expectedly, porosity (<1%) and permeability (<1mD) values are as bad as guessed from the SEM images. Absence of macroscopic pores (i.e. other than fractures), and tightness of micrite crystals explain the poor reservoir quality. Another important feature of C03 is partly-open fractures and cracks crossing the sample.

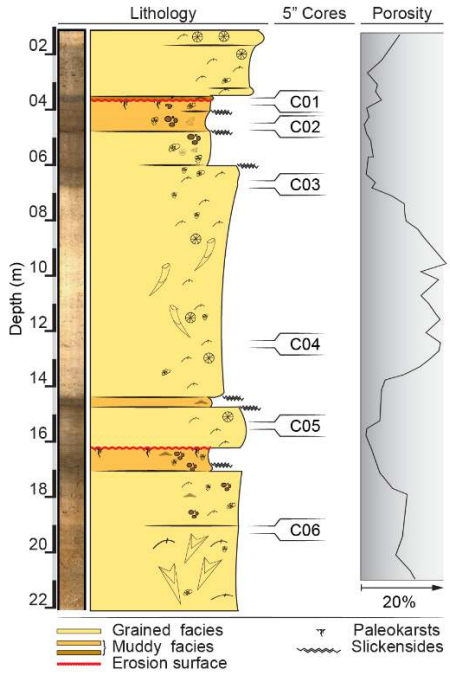

Figure 1. Synthetic lithology and porosity logs of studied formations, and localization of cores C01 to C06.

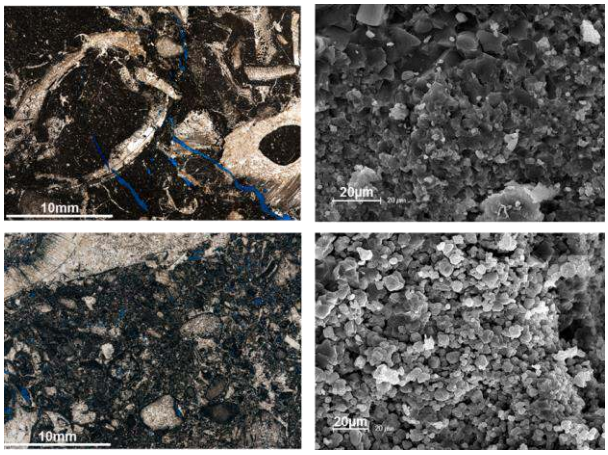

Figure 2. Stained thin-sections (left) and SEM imaging (right) of cores C03 (top) and C04 (bottom). Notice the contrast in micrite crystals shapes and inter-crystalline pores between the non-porous C03 and porous C04.

The footprint of fracturing, is visible on thin sections, since fractures' porosity, significantly increases the overall porosity.

C04 represents the most porous interval in studied formation, its porosity is about 15% but may reach up to 20%, and its permeability ranges from 2 to 3.5mD. C04 facies is a bioclastic grainstone to rudstone with large rudists' fragments. The thin sections show grain size ranging from 200µm, for the finest, to 2mm for the largest (Figure 2). Macroscopic pores both moldic and vuggy, are frequent, but the overall porosity, is dominated by intercrystalline porosity within the micrite (microporosity). SEM images show that micrite crystals are larger than that of the non-porous samples. The micrite crystals are loosely packed, euhedral, and heterogeneous in size, (i.e. 1 to 5µm), while intercrystalline pores are abundant, and relatively well connected because of either poor sorting, or low contact area between micrite crystals.

Material and methods:

Ultrasonic measurements were carried out in two parts. Firstly, the 5" cores were preliminarily saturated, then flooded in an acoustic tank, 20°C tap water was used during all steps. We do not give an extensive description of the experimental set up in this abstract, but Figure 3 shows the experiment.

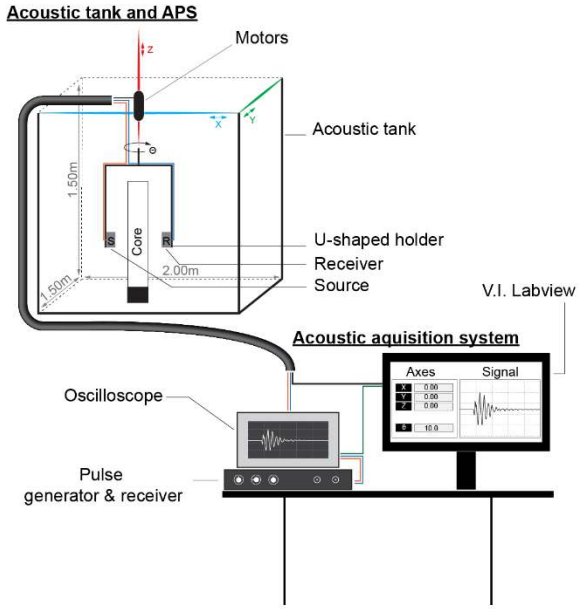

Figure 3. Experimental set up for ultrasonic analyses on 5" cores. The instrumentation included: 250-kHz IMASONIC immersion transducers, oscilloscope TEKTRONIX-DPO4034, pulse generator–receiver PANAMETRICS-5058PR.
During acquisition transducers rotate around the sample. The rotation step (ΔΘ), is 5°, and for a given transversal-section, 72 signals (stacked: ×64) are recorded. After that the transducers are moved 1cm up (ΔZ=1cm), then the process is repeated.

Secondly, three 1.5" mini-cores (plugs) were drilled out of each 5" core. The mini-cores were taken in directions normal, parallel, and 45° to beddings, then wave velocities were measured using pairs of P- and S-wave PANAMETRICS ultrasonic transducers (1MHz). Good surface contact was ensured by using a thin lead foil at each interface, and by applying surface contact force using a vise.

The data were investigated using model of transversely isotropic (TI). For TI materials, the stiffness tensor (C_{IJ}) written in Voigt's notation, requires only five independent components to fully describe the elasticity (equation (1)).

$$C_{IJ} = \begin{pmatrix} c_{11} & c_{12} & c_{13} & & & \\ c_{12} & c_{11} & c_{13} & & & \\ c_{13} & c_{13} & c_{33} & & & \\ & & & c_{44} & & \\ & & & & c_{44} & \\ & & & & & c_{66} \end{pmatrix}, \quad c_{66} = \frac{c_{11} - c_{12}}{2} \qquad (1)$$

After equation (2), components of C_{IJ} can be obtained from the density (ρ), and five velocity measurements including both quasi-longitudinal (Vp), and pure-shear (Vsh) phase-velocities (Mavko, Mukerji, and Dvorkin 2009).

$$\begin{aligned} c_{11} &= \rho Vp^2_{(90°)} \\ c_{33} &= \rho Vp^2_{(0°)} \\ c_{44} &= \rho Vsh^2_{(0°)} \\ c_{66} &= \rho Vsh^2_{(90°)} \end{aligned} \qquad c_{13} = -c_{44} + \begin{pmatrix} 4\rho^2 Vp^4_{(45°)} - 2\rho Vp^2_{(45°)} \\ \times (c_{11} + c_{33} + 2c_{44}) \\ + (c_{11} + c_{44})(c_{33} + c_{44}) \end{pmatrix}^{1/2} \qquad (2)$$

Thomsen (1986) definition for weak TI media states the conditions $|\varepsilon| \ll 1$ and/or $|\gamma| \ll 1$ must hold, and the author also suggested an approximation of P-wave phase velocity Vp(θ) for weak TI material, using P-wave velocity (noted α in equation (3)), and three constants, namely ε, γ, and δ, given by following formulas:

$$Vp(\theta) \approx \alpha\left(1 + \delta \sin^2\theta \cos^2\theta + \varepsilon \sin^4\theta\right)$$

$$\alpha = \sqrt{c_{33}/\rho} \quad \varepsilon = (c_{11} - c_{33})/2c_{33} \quad \gamma = (c_{66} - c_{44})/2c_{44} \qquad (3)$$

$$\delta = \left((c_{13} + c_{44})^2 - (c_{33} - c_{44})^2\right) / \left(2c_{33}(c_{33} - c_{44})\right)$$

For mini-cores, components of C_{IJ} were computed using equation(2). Regarding mini-cores size, any anisotropy at this scale is related either to matrix, or micro-cracks, but not to macroscopic fractures. For 5" cores we fitted Vp(θ) models, using equation (3), onto velocity data for each transversal section. This gave us an estimation of quantities α, ε, and δ. Finally, these quantities (Thomsen's parameters) and/or the stiffness coefficients, were compared to results obtained on mini-cores (1.5"), cores (5"), and crosshole survey (meter to multi-meter).

Results and Discussion:

The results of the "mini-core approach" are given in Table 1. C_{IJ} components are nearly identic for non-porous samples (i.e. C01, C02, C03, and C05), whereas they are significantly lower for porous ones (i.e. C04, C06). This values are consistent with C_{IJ} components obtained from 1" mini-cores, and crosshole-ultrasonic survey (see Baden et al., *@submitted article*, Fournier et al. (2014), and #1 Baden et al., *@SEG2017*), but are significantly higher than that from Bereš et al. (2013), for measurements at seismic frequencies (Table 2).

Focusing on C03 and C04 (Table 1), one can see that shear anisotropy (γ) is <1%, therefore it is negligible. Conversely, ε is very low for C03 (2.3%), but is significant for C04, where it reaches ~12%. This results emphasizes that at matrix scale, porous samples can show significant P-wave anisotropy, whereas not-porous ones are nearly isotropic. Consequently, intercrystalline pores may be responsible for most of observed anisotropy.

Table 1. Results of the analyses on mini-cores.

	C01	***C02***	***C03***	***C04***	***C05***	***C06***
C_{11}	107,9	110,3	109,0	29,5	101,5	56,6
C_{13}	41,6	55,5	29,1	7,5	61,3	21,8
C_{33}	107,1	100,7	104,3	38,6	106,8	58,2
C_{44}	28,6	28,9	27,6	10,9	26,8	16,6
C_{66}	28,7	29,0	27,5	10,7	26,7	16,6
ρ	2649	2660	2618	2306	2650	2388
ε	0,004	0,048	0,023	-0,118	-0,025	-0,014
γ	0,003	0,001	-0,002	-0,008	-0,002	-0,001
δ	-0,074	0,137	-0,167	-0,201	0,080	-0,053

$C_{IJ} \times 10^9$; ρ (kg/m^3)

Up-scaling analyses to 5" cores, one can see in most cases, P-wave velocities are low anisotropic in the transverse plane, i.e. ε range between ±5%, for given transversal-section, (Figure 4, and Figure 5). When particular features such as fractures or large cemented-bioclasts (e.g. recrystallized corals and rudists) occur, P-wave velocities become clearly anisotropic, and ε can reach up to ±20%. CT scan imaging show that in non-porous samples (e.g. C03) anisotropy (in transverse plane) is related to fractures and cracks only, and its magnitude can be related to either high density of thin cracks, or thick single-fracture.

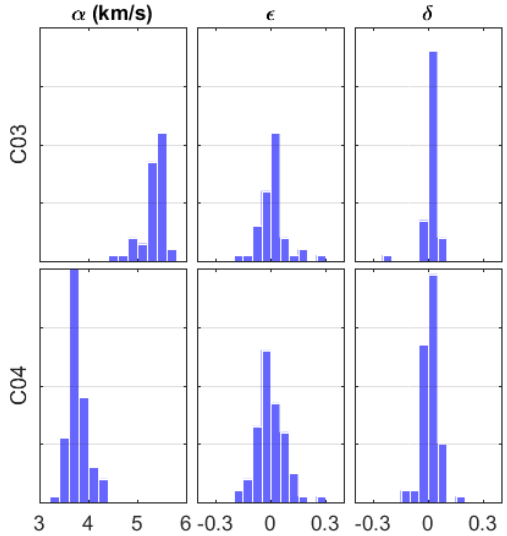

Figure 4. Estimation of α, ε, and δ using curve fitting of Vp(θ) on the 5" cores data (cf. transversal-section). The count is given by ordinate axes [0, 40].

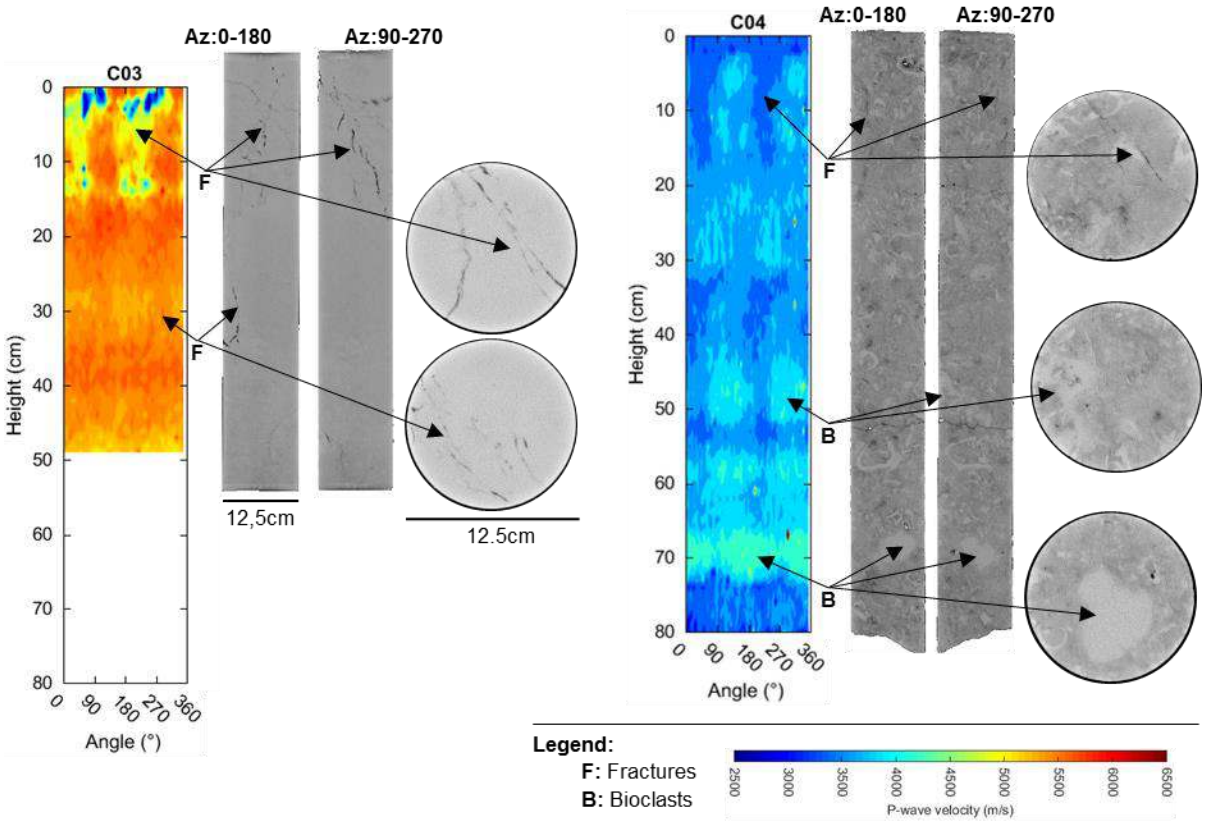

Figure 5. P-wave velocity maps and CT scan images of C03 & C04. Maps are 2D version (i.e. unrolled) of the 3D acquisition grid. The CT scan slices (longitudinal, and transversal) are commented to emphasize impact of bioclasts and fractures on recorded velocities. The gray level gives an idea of actual density, e.g. white→dense→non-porous.

In porous sample (e.g. C04) anisotropy in transverse plane can be related to either density contrasts within porous matrix, or inclusion of macro-fossils (Figure 5). In first case, P-wave velocity can stay close to mini-cores values, but in the second case it can be significantly higher than that of matrix alone.

Table 2. Ranges for C_{IJ} ($\times 10^9$) in Urgonian limestone.

	[1]	[2]	[3]	[4]
C_{11}	44,9 - 36,9	96,3 - 39,5	110,3 - 29,5	110,4 - 26,8
C_{13}	19,7 - 18,3	43,5 - 12,1	61,3 - 07,5	52,7 - 09,2
C_{33}	69,2 - 65,9	93,5 - 35,3	107,1 - 38,6	C_{11}
C_{44}	19,7 - 18,3	28,7 - 15,3	28,9 - 10,9	34 - 07,9
C_{66}	15,4 - 14,8	26,7 - 12,3	29 - 10,7	C_{44}

[1] Bereš et al., (2013); **[2]** Baden et al. (submitted);
[3] This study (mini-cores: 1.5"); **[4]** Fournier et al., (2014).

Conclusion:

Our multi-scale approach integrated data from centimeter-scale (1", 1.5" mini-cores), decimeter-scale (5" cores), multi-meter (ultrasonic crosshole), and hectometer-scale (seismic), these data were collected using frequency ranges suitable for the scales investigated, i.e. 1MHz, 250kHz, 50kHz, and 1-100Hz, respectively.

Although anisotropy is measureable at every scales, causes of that anisotropy can vary, or interfere with each other, according to scale. The data showed that porous matrix could be weakly anisotropic, at plug-scale, inter-crystalline pores may be the reason (Fournier et al. 2014). At centimeter-scale, patchy distribution of some physical properties (e.g. density) and/or local fractures/cracks distribution, produce anisotropy in the transverse plane, meaning similar consequences may be expected in the vertical plane. Effects of minerals/pores orientation and local fractures distribution are also visible at multi-meter scale, they are expressed by anisotropy being tightly correlated to beddings. However, when fracturing dominates signal from matrix anisotropy may be overlapped by fracture-related anisotropy. As shown by lack of correlation between C_{IJ} components from seismic-scale measurements, and laboratory to multi-meter scale ones (Table 2). Therefore scale effect must be handled carefully in anisotropy analyses, especially for carbonate formations.

Acknowledgements:

This works were supported by two Research programs: H–CUBE project (ANR-12-SEED-0006), D. Baden's PhD grant; and ALBION-HPMSCa project, funded by TOTAL.

Bibliography (not to be included in the abstract)

Bereš, Ján, Hermann Zeyen, Guy Sénéchal, Dominique Rousset, and Stéphane Gaffet. 2013. "Seismic Anisotropy Analysis at the Low-Noise Underground Laboratory (LSBB) of Rustrel (France)." *Journal of Applied Geophysics* 94: 59–71. doi:10.1016/j.jappgeo.2013.04.008.

Borgomano, Jean, Jean-Pierre Masse, Mukerrem Fenerci-Masse, and François Fournier. 2013. "Petrophysics of Lower Cretaceous Platform Carbonate Outcrops in Provence (SE France): Implications for Carbonate Reservoir Characterisation." *Journal of Petroleum Geology* 36 (1): 5–42.

Fournier, F, and J Borgomano. 2009. "Critical Porosity and Elastic Properties of Microporous Mixed Carbonate-Siliciclastic Rocks" 74 (2).

Fournier, François, Philippe Leonide, Kévin Biscarrat, Arnaud Gallois, Jean Borgomano, and Anneleen Foubert. 2011. "Elastic Properties of Microporous Cemented Grainstones." *Geophysics* 76 (6): E211–26.

Fournier, François, Philippe Léonide, Luuk Kleipool, Renault Toullec, John J.G. Reijmer, Jean Borgomano, Thomas Klootwijk, and Jeroen Van Der Molen. 2014. "Pore Space Evolution and Elastic Properties of Platform Carbonates (Urgonian Limestone, Barremian–Aptian, SE France)." *Sedimentary Geology* 308 (July). Elsevier B.V.: 1–17.

Jeanne, Pierre. 2012. "Architectural, Petrophysical and Hydromechanical Properties of Fault Zones in Fractured-Porous Rocks: Compared Studies of a Moderate and a Mature Fault Zones (France)." Aix-Marseille Université.

Jeanne, Pierre, Yves Guglielmi, and Frédéric Cappa. 2012. "Multiscale Seismic Signature of a Small Fault Zone in a Carbonate Reservoir: Relationships between VP Imaging, Fault Zone Architecture and Cohesion." *Tectonophysics* 554–557 (July): 185–201.

———. 2013. "Dissimilar Properties within a Carbonate-Reservoir's Small Fault Zone, and Their Impact on the Pressurization and Leakage Associated with CO2 Injection." *Journal of Structural Geology* 47 (February). Elsevier Ltd: 25–35.

Jeanne, Pierre, Yves Guglielmi, Juliette Lamarche, Frédéric Cappa, and Lionel Marié. 2012. "Architectural Characteristics and Petrophysical Properties Evolution of a Strike-Slip Fault Zone in a Fractured Porous Carbonate Reservoir." *Journal of Structural Geology* 44 (1): 93–109.

Leonide, Philippe, Jean Borgomano, Jean-Pierre Masse, and Stefan Doublet. 2012. "Relation between Stratigraphic Architecture and Multi-Scale Heterogeneities in Carbonate Platforms: The Barremian–lower Aptian of the Monts de Vaucluse, SE France." *Sedimentary Geology* 265–266 (July): 87–109.

Léonide, Philippe, François Fournier, John J.G. Reijmer, Hubert Vonhof, Jean Borgomano, Jurrien Dijk, Maelle Rosenthal, Manon van Goethem, Jean Cochard, and Karlien Meulenaars. 2014. "Diagenetic Patterns and Pore Space Distribution along a Platform to Outer-Shelf Transect (Urgonian Limestone, Barremian–Aptian, SE France)." *Sedimentary Geology* 306 (June). Elsevier B.V.: 1–23.

Mavko, Gary, Tapan Mukerji, and Jack Dvorkin. 2009. *The Rock Physics Handbook*. 2nd ed. Cambridge University Press, Cambridge.

Thomsen, Leon. 1986. "Weak Elastic Anisotropy." *Geophysics* 51 (10): 1954–66.